

Formation of copper electrodeposits on an untreated insulating substrate

Min-Zhe Zhang¹, Yuan Wang¹, Guang-Wei Yu^{1,2}, Mu Wang^{1,3,4},
Ru-Wen Peng¹, Yu-Yan Weng¹ and Nai-Ben Ming¹

¹ National Laboratory of Solid State Microstructures and Department of Physics, Nanjing University, Nanjing 210093, People's Republic of China

² Institute of Crystal Materials, Shandong University, Jinan 250100, People's Republic of China

³ International Centre of Quantum Structures, Institute of Physics, Chinese Academy of Sciences, Beijing 10080, People's Republic of China

E-mail: muwang@nju.edu.cn

Received 1 July 2003

Published 16 January 2004

Online at stacks.iop.org/JPhysCM/16/695 (DOI: 10.1088/0953-8984/16/4/016)

Abstract

We report here the electrodeposition of copper on an insulating glass substrate without introducing additives into the electrolyte and/or metallic clusters on the surface of the substrate. The deposit morphology, which varies from compact film to dense-branching patterns, can be achieved by changing the concentration and pH of the electrolyte, and the electric current in electrodeposition. The grain size of the electrodeposits is analysed for various growth conditions. We find that finer copper grains can be easily achieved at large electric current, high pH and low electrolyte concentration. We explain, using the theory of nucleation, why a metallic layer may develop horizontally over an insulating glass plate.

1. Introduction

The importance of copper for the next generation of on-chip interconnection has been well established due to the discovery that copper wiring has advantages over Ti/Al(Cu) wiring such as lower resistance, higher allowed current density and increased scalability [1–3]. Much effort has been devoted to copper electrodeposition in recent years due to both the technological requirements and the scientific interests [4–15]. To achieve a robust copper film on a solid substrate by electrochemical deposition, usually a special electrolyte solution has to be prepared, into which surface-active additives are introduced. Instead of using additives, an alternative method is to modify the substrate surface physically by coating it with a layer of gold clusters [16, 17]. The density of the gold clusters on the substrate is below the threshold value of percolation, so the surface remains non-conductive. The gold clusters provide favourable sites for nucleation on the glass substrate. Yet it has recently been found that the gold nanoclusters

⁴ Author to whom any correspondence should be addressed.

tend to form an alloy with the metal that is to be deposited [18], which is not desirable for applications such as sensors. For the scenario where organic additives are introduced, the electrolyte usually contains functional sulfur and/or nitrogen groups that tend to adsorb on the surface of the substrate, thereby suppressing the metal deposition rate. The adsorption and the associated inhibition finally lead to smaller grains of the metal deposit. However, the trapped organic additives in the electrodeposits may affect the mechanical and/or electrical properties of the electrodeposits. Therefore, it is worth exploring different ways of depositing metal electrochemically on an insulating substrate, without using either additives in the electrolyte or metal clusters (such as gold clusters [16, 17]) on the substrate surface.

In this paper we report our experimental studies on the electrodeposition of copper on an insulating glass substrate. The deposit morphology varies from compact to dense-branching patterns by changing the electrolyte concentration, the pH of the electrolyte and the electric current. Using the theory of nucleation and crystallization, we explain why the metal can be deposited on an insulating glass plate and why the microscopic morphology of the copper deposit depends on concentration, pH and electric current.

2. Experiments and results

Our experiments were carried out in a thin electrodeposition cell made of two carefully cleaned glass plates. Slices of copper foil (18 μm in thickness, 99.9% pure) were used as electrodes. The copper foils also acted as spacers between the upper and lower glass plates of the electrodeposition cell. The foil electrodes were fixed on the bottom glass plate by a very thin layer of epoxy resin. In our experiments, the electrodes were straight and parallel and the separation between the two electrodes was 6 mm. The electrodeposition cell was filled by capillary action with CuSO_4 electrolyte which was confined in the space between the upper and lower glass plates and the electrodes. The electrolyte solution was prepared by dissolving the analytical reagent CuSO_4 in de-ionized, ultrapure water (electrical resistivity 18.7 $\text{M}\Omega\text{ cm}$). The concentration of the electrolyte was selected to be between 0.03 and 0.13 M. The glass plates were cleaned carefully with a solution of concentrated H_2SO_4 (98%) and $\text{K}_2\text{Cr}_2\text{O}_7$. The glass plates were then rinsed thoroughly with ultrapure water and dried in nitrogen gas. The deposition cell was placed in a isothermal chamber, where the temperature was kept at 30 $^\circ\text{C}$, which was guaranteed by a programmable thermostat (Polystat, USA). Detail of the structure of the experimental system was similar to that reported in [19]. The electrodeposits were observed *in situ* by an optical microscope (Leitz, Orthoplan-pol, Germany). The microstructure of the electrodeposit was further characterized by a field emission scanning electron microscope (LEO 1530VP, Germany) and a transmission electron microscope (Philips Tecnai F20, the Netherlands). In the electrodeposition, a constant current was applied across the electrodes by a DC power supply accurate to $\pm 1\ \mu\text{A}$.

When the separation between the upper and lower glass plates was large, as reported in previous studies [7–12], the ramified electrodeposits were normally floating in the electrolyte. Yet we found that, by decreasing the thickness of the electrolyte layer, the probability that electrodeposits grew on the glass plates became higher. When the separation was decreased to about 20 μm , the chance that the electrodeposits stuck on the glass plate could reach about 80%. The reproducibility of directly coating the glass substrate in electrodeposition also depended on the electric current, the electrolyte concentration and the surface energy of the substrate⁵. In most cases, the copper branches were deposited firmly on the glass surface and the coating could not be removed from the substrate without deliberate scraping.

⁵ The surface energy of a selected substrate depends on whether the substrate is clean.

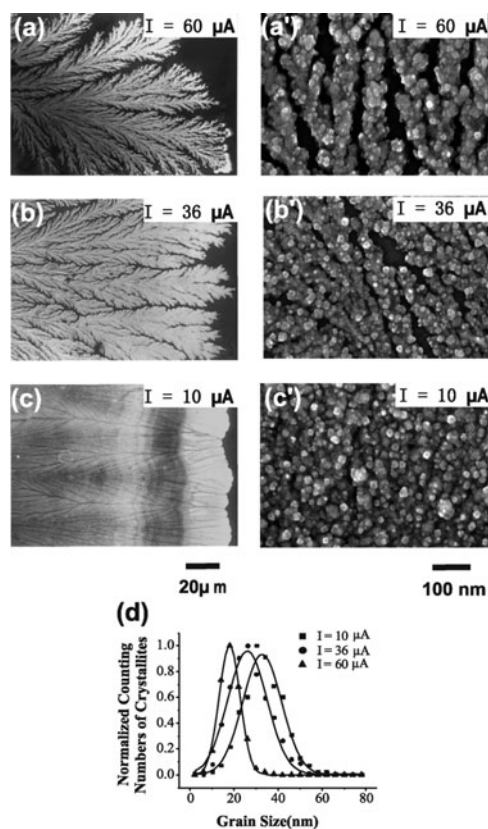


Figure 1. Copper electrodeposits on the glass substrate. The electrolyte concentration of CuSO_4 was 0.07 M and $\text{pH} = 4.25$. (a) and (a') show the electrodeposit grown at 60 μA . The deposits shown in (b) and (b') are generated at 36 μA . When the electric current is decreased to 10 μA , a compact, film-like deposit is formed ((c) and (c')). (d) The distribution of the grain size at different applied electric currents. The distribution counts of the crystallites have been normalized.

Our experiments showed that the morphology of the copper deposit varied with electric current and electrolyte concentration and pH. We first carried out the experiments in a 0.07 M aqueous solution of CuSO_4 ($\text{pH} = 4.25$) with constant electric currents of 60, 36 and 10 μA . When the electric current was high, the deposit branches were ramified, as shown in figure 1(a). By lowering the electric current to 36 μA , the deposit branches became more dense and the separation between the branches became narrower (figure 1(b)). Further decrease of the electric current to 10 μA led to a compact, film-like deposit, as illustrated in figure 1(c).

Corresponding to the morphological change on a macroscopic scale, microscopically the deposit morphology also differed for different electric currents. As illustrated in figures 1(a')–(c'), when the electric current was reduced, the deposit filled up more space. The size distribution of the copper grains was statistically counted, based on the scanning electron microscope (SEM) measurements. The size of a copper crystallite was determined in the following way. Once a crystallite was selected, the mass-centre of the area that the crystallite occupied was determined, and hence the radius of gyration was obtained. This radius of gyration was used to characterize the crystallite size. About 1000 crystallites were randomly selected and measured for each experiment in order to diminish the experimental errors. The

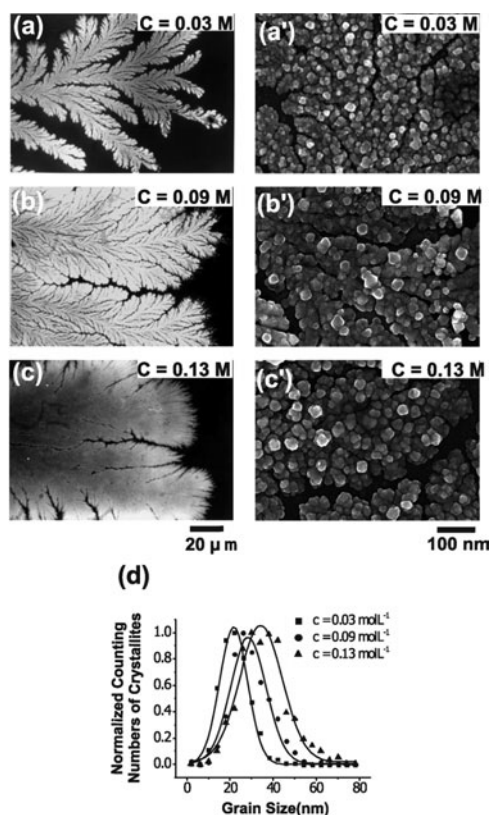


Figure 2. The dependence of electrodeposit morphology on electrolyte concentration. (a)–(c) show the deposit observed with optical microscopy and (a')–(c') illustrate the corresponding microscopic details observed with a field emission SEM. (d) The distribution of grain size for different electrolyte concentrations.

measured data were fitted by a Gaussian curve. It can be seen in figure 1(d) that at higher electric current the crystallites were smaller than those formed at lower electric current.

The electrolyte concentration affected both macroscopic and microscopic morphology of the copper deposit. As shown in figures 2(a)–(c), by increasing the electrolyte concentration, the deposit morphology changed gradually from a ramified, dense-branching pattern to a more compact finger-like pattern. The deposit branches consisted of tiny, closely packed grains when the electrolyte concentration was 0.03 M, as illustrated in figure 2(a'). Statistics showed that most of the crystallites had sizes around 20 nm (figure 2(d)). When the concentration increased to 0.09 M, as indicated in both figures 2(b) and (b'), the width of the branches increased evidently and the grains in the branches also became larger. In this case the distribution of grain size had a maximum around 28 nm. When the electrolyte concentration was further increased, we observed that, on average, the grains enlarged further. As demonstrated in figures 2(c') and (d), when the concentration reached 0.13 M, the peak in the crystallite size distribution was around 35 nm.

Figure 3 demonstrates the dependence of deposit morphology on the pH of the electrolyte. In our experiments, the pH of the electrolyte varied between 2.02 and 4.64. We found that on a macroscopic scale the deposit branches seemed less sensitive to the variation of pH. As illustrated in figures 3(a)–(c), the deposit remained dense-branching, even though the pH had

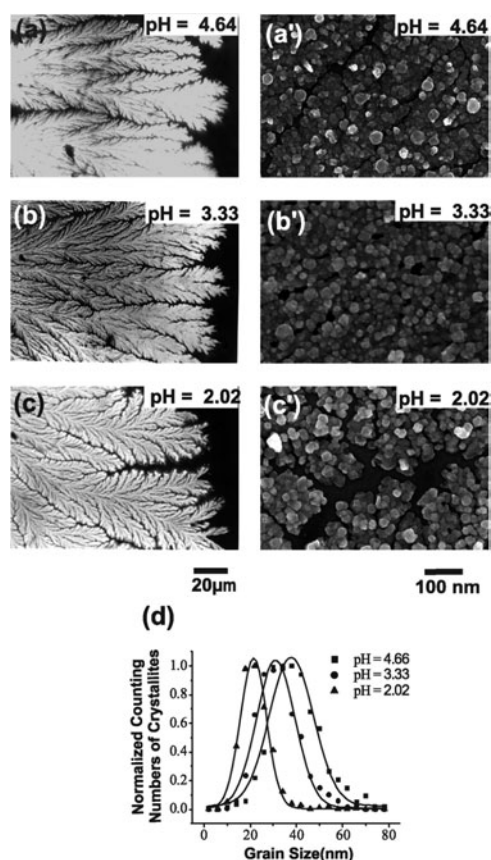


Figure 3. The morphology of the electrodeposit grown at different pH values of the electrolyte. (a)–(c) show the deposit observed with optical microscopy, and (a')–(c') illustrate the corresponding SEM micrographs of the deposits. (d) The distribution of grain size at different pH values of the electrolyte solution.

been modified by more than a factor of two. Microscopically, however, the differences could be clearly identified. Figures 3(a')–(c') and (d) demonstrated that, by decreasing the pH from 4.64 to 2.02, the maximum of the size distribution shifted from 21 to 38 nm, indicating that a more acidic environment could generate larger crystallite grains.

We also carried out electron diffraction on the electrodeposits generated at different pH, and studied the change of the chemical components and microstructure. Figure 4(a) shows the electron diffraction on the electrodeposits grown at pH = 2.02. The diffraction rings indicated that the electrodeposits were polycrystalline. By indexing the diffraction rings we concluded that the electrodeposits were made of copper. By careful inspection of figure 4(a) one may still find a few separate diffraction spots of Cu_2O (220), suggesting that the amount of Cu_2O crystallite in the electrodeposits is very low. Figure 4(b) illustrates the electron diffraction of the electrodeposits grown at pH = 3.33. Comparing with figure 4(a), in addition to the diffraction of copper, the diffraction from Cu_2O (111) and (220) could be easily identified. A further increase of pH increased the amount of Cu_2O crystallite even more. As indicated in figure 4(c), when the pH of the electrolyte reached 4.64, those rings corresponding to Cu_2O became very evident. We therefore conclude that the concentration of Cu_2O crystallites inside the electrodeposits increases when the pH of the electrolyte is increased.

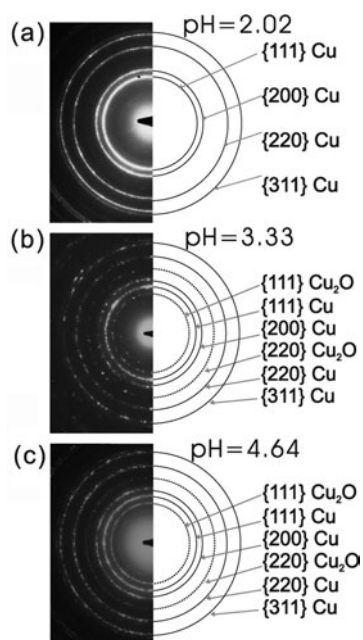


Figure 4. The electron diffraction pattern of the deposits generated in electrolytes with different pH values. (a) The diffraction rings of the electrodeposits for pH = 2.02, amongst which just a few separated dots corresponding to Cu_2O can be identified. (b) The electron diffraction of the electrodeposits for pH = 3.33. The diffraction rings corresponding to Cu_2O can be easily seen. (c) When the pH of the electrolyte is increased to 4.64, clear and continuous rings corresponding to Cu_2O appear, suggesting that the amount of Cu_2O crystallites has been increased significantly.

We also carried out electrodeposition with the same pH (pH = 4.25) but with different electrolyte concentrations (the concentration varied from 0.03 to 0.13 M while the current was fixed at $36 \mu\text{A}$) and different electric currents across the electrodes (the current varied from 10 to $60 \mu\text{A}$ with concentration fixed at 0.07 M). By mapping the electrodeposits with energy dispersive x-ray analysis in the scanning electron microscope, we expected that we would be able to distinguish the difference on the Cu_2O distribution over the surface of the electrodeposits. However, we did not find much difference on the Cu_2O content in the samples generated under different experimental conditions. This may imply that the amount of Cu_2O crystallites in the electrodeposits may not be very sensitive to the changes in the applied electric current or electrolyte concentration in our experiments.

3. Discussions

In previous experiments, the electrodeposits were usually floating in the electrolyte [7–10, 12], which could be easily disturbed by convective movement of the fluid around the electrodeposits. The major difference between our current results and previous ones is that, in our experiment, the metallic branches can be deposited on an insulating glass plate without special treatment of the glass surface. It is worth finding out why the metallic crystallites prefer to nucleate on an insulating glass plate. We suggest that there exist two scenarios for nucleating copper crystallite on the growth front, as schematically shown in figure 5. In one case, the crystallite initiates on the copper deposit via heterogeneous nucleation (scenario 1). In the other case,

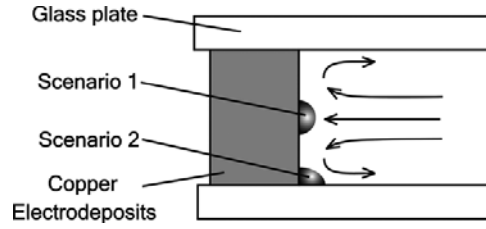


Figure 5. A schematic diagram to show the sites of nucleation on the growth front and the streamlines in front of the electrodeposit.

the crystallite nucleates at the concave corner of the copper deposit and the glass surface (scenario 2). If electrodeposition continues via scenario 1, then the electrodeposits will form an aggregate floating in the electrolyte. If, however, scenario 2 dominates, copper will coat the substrate (glass plate). In electrochemical deposition, the crystallographic orientation of the crystallites is normally random (indeed this can be seen in figure 4) and the copper nucleus does not possess the same crystallographic orientation as the substrate. This situation is common when the growth is far from equilibrium and some impurities exist on the growing interface. Suppose the interfacial energy of copper and electrolyte is denoted as φ , and the interfacial energy of the copper nucleus and the copper substrate is only a small fraction of φ . Define α as a small constant, which approaches zero only for epitaxial growth (i.e. the case where the orientation of the nucleus is the same as the substrate). Then the interfacial energy of the copper nucleus and the copper substrate can be represented as $\alpha\varphi$. The contact angle of the nucleus and the deposit, θ , can be expressed as $\cos\theta = 1 - \alpha$. It follows that the energy barrier for nucleation in scenario 1 can be written as [20]

$$\Delta G_1^* = \frac{\varphi^2 \Omega}{|\Delta g|} [\arccos(1 - \alpha) - (1 - \alpha)\sqrt{2\alpha - \alpha^2}],$$

where Δg is the change of the free energy required for a copper ion to become an atom in electrocrystallization, and Ω is the volume of the atom. The detailed deduction of ΔG_1^* will be given separately [20]. For scenario 2, the substrate is asymmetric: one part of the substrate is copper, whereas the other part of the substrate is glass. Suppose the surface energy of the glass substrate and the electrolyte is ξ , and interfacial energy of the copper nucleus and the glass is γ_{cs} . We assume that γ_{cs} is only a fraction of φ , $\gamma_{cs} = \chi\varphi$, where χ is a parameter less than unity. The radius of curvature of the nucleus is r . The energy barrier for nucleation at the concave corner (here for simplicity we take the concave corner as 90°) has the form [20]

$$\Delta G_2^* = \frac{\varphi^2 \Omega}{2|\Delta g|} \left(\arccos(1 - \alpha) + \arccos\Theta - \frac{\pi}{2} - (\sqrt{2\alpha - \alpha^2} - \Theta)(1 - \alpha) - \left[\sqrt{1 - \Theta^2} + \alpha - 1 \right] \Theta \right) = \frac{\varphi^2 \Omega}{|\Delta g|} \frac{\Lambda}{2},$$

where $\Theta = \frac{\xi}{\varphi} - \chi$. The difference between these two energy barriers, δ , can be expressed as

$$\delta = \Delta G_2^* - \Delta G_1^* = \frac{\varphi^2 \Omega}{|\Delta g|} \left[\frac{\Lambda}{2} - \arccos(1 - \alpha) + (1 - \alpha)\sqrt{2\alpha - \alpha^2} \right].$$

The sign of δ decides which site will be more energetically favourable for nucleation. Our calculations indicate that δ remains negative unless α and Θ are very small. Small α means that the electrodeposition of copper on copper aggregate is virtually an epitaxial process, which is clearly not the case in our experiment. As a matter of fact, the random crystallites shown in

figure 2 indicate that in our system α should not be small. The value Θ equates to the cosine of the wetting angle of copper on glass substrate. The fact that copper can be deposited on a glass surface indicates that Θ is not small. Instead, Θ should be close to unity. Therefore we conclude that δ should be negative for most cases, which means that nucleation at the concave corner (scenario 2) is thermodynamically favoured in electrodeposition.

We need to point out, however, that whether an electrodeposition can be experimentally observed depends on the nucleation rate, which is defined as the number of nuclei that may develop into crystallites in unit time and unit volume. The nucleation rate depends on both the energy barrier of nucleation ΔG and the probability that a nucleus catches the ions from the fluid. The steady state nucleation rate I can be expressed as

$$I = \omega^* \Gamma Z_1 e^{-\frac{\Delta G^*}{kT}},$$

where Z_1 is the concentration of cations near the electrodeposit, Γ is known in the literature as the Zeldovich factor, and ω^* is the frequency with which the critical nucleus collects the cations [21]. It is known that, when the electrodeposition cell is thick, convection caused by the external fields will be strong and streamlines such as those shown in figure 5 are to be expected. At the same time, the middle part of the deposit faces the flux of cations, hence ω^* is larger in this region. On the hand, those parts at the concave corner of the copper deposit and the glass plate feel a flux moving away from the deposit, which implies that the nucleus will find it more difficult to catch cations, compared to scenario 1. Consequently, ω^* becomes smaller at the concave corner. The difference between ω^* at these two sites is related to the thickness of the electrodeposition cell. Thermodynamically, even though the nucleation barrier at the concave corner is lower, the local nucleation rate on the glass plate may not be high due to the smaller ω^* at the concave corner in the thick cell. By decreasing the cell thickness, convection is strongly suppressed and the ion transfer is mainly driven by the electric migration and diffusion. In addition, ω^* becomes more homogeneous over the whole deposit interface. Hence the thermodynamic effect may dominate the electrodeposition. Consequently, copper crystallites may coat the glass plate.

From the above discussion, one may conclude that there are different approaches to depositing copper on a solid substrate. One way is to modify the surface energy of the glass plate and to decrease ΔG_2^* , which corresponds to that proposed by Fleury *et al* [16, 17]; an alternative way is to decrease the thickness of the electrolyte layer. Then, the nucleation rate on the glass plate is increased, as we report in this paper and is also shown in [15] and [19].

The distribution of grain sizes as a function of the applied electric current can be understood based on the theory of nucleation [21]. It is known that the critical size for nucleation, r^* , below which the aggregate will spontaneously disappear due to fluctuation, relates to Δg (the change of free energy required for a copper ion to become an atom in electrocrystallization) as follows:

$$r^* = \frac{\varphi \Omega}{|\Delta g|}.$$

When the electric current is high, the growth is further from equilibrium and $|\Delta g|$ is larger. Consequently, the critical size for nucleation is smaller and the copper crystallites will be smaller. This tendency has indeed been observed (figure 1(d)).

The relationship between the grain size distribution and the electrolyte concentration can be explained as follows. It is known that the conductivity of the electrolyte of CuSO_4 depends on the concentration. The electrolyte is more conductive when the electrolyte concentration is higher. Therefore, in order to achieve the same electric current in galvanostatic mode, the voltage applied across the electrodes should be different for different electrolyte concentrations: the voltage is higher for lower electrolyte concentration and lower for higher electrolyte

concentration. This means that, in a galvanostatic scenario, the driving force for nucleation and crystallization is higher when the electrolyte concentration is lower, and the driving force becomes smaller for higher electrolyte concentration. As we mentioned earlier, the size of the copper nucleus is smaller and the nucleation rate is higher when the driving force $|\Delta g|$ is high. Once sufficient nuclei are induced, competition for nutrient supply confines the growth of these crystallites. Therefore, at a lower concentration, the copper crystallites are smaller due to the smaller initial nucleus size and the limited growth thereafter; for a higher electrolyte concentration, the crystallites are larger due to the lower nucleation rate. This is consistent with figure 2.

It is noteworthy that the crystallites of copper in the deposit branches cannot keep growing continuously. Up to a certain size the growth stops and new nucleus appears. This behaviour may be due to the existence of Cu_2O during electrodeposition in aqueous electrolyte solution, as illustrated in figure 4. In fact, Cu_2O coexists with copper in electrodeposition [15, 22, 23], which may act as impurity to poison the growth of copper grains. Cu_2O can be dissolved in an acidic environment. When the pH of the electrolyte is sufficiently low, Cu_2O will not survive. Therefore, in an acidic solution, the growth of copper crystallites will last for a longer time and the copper crystallite may reach a larger size. When the electrolyte is less acid, more Cu_2O will be generated, which will quickly block the growth of copper crystallite. This explains the tendency shown in figure 3(d), where crystallites are larger at low pH.

4. Conclusion

We report in this paper an experimental observation that copper can be electrodeposited on an insulating glass substrate without introducing additives into the electrolyte solution and without modifying the glass surface with metallic clusters. Whether a layer of copper crystallites can be electrodeposited on glass substrate depends on both the nucleation barrier (thermodynamic factor) and the local nucleation rate (kinetic factor). When the thickness of the electrolyte layer becomes sufficiently small (and electroconvection and natural convection are strongly suppressed), the thermodynamic factor will dominate the interfacial process. Hence copper will coat the glass substrate. Both the deposit morphology and the copper crystallite vary as a function of electrolyte concentration, the pH of the electrolyte and the applied electric current. Our experiments show that finer grain size can be achieved at larger electric current, higher pH of the electrolyte and lower electrolyte concentration.

Acknowledgments

This work was supported by the grants from the Ministry of Science and Technology of China (No. G1998061410) and the National Science Foundation of China (No. 10374043 and No. 10021001). The discussions with Dr V Fleury are also acknowledged.

References

- [1] Edelstein D, Heidenreich J, Goldblatt R, Cote W, Uzoh C, Lustig N, Roper P, McDevitt T, Motsiff W, Simon A, Dukovic J, Wachnik R, Rathore H, Schulz R, Su L, Luce S and Slattery J 1997 *IEEE Technical Digest on International Electronic Devices Meeting* (Washington, DC: IEEE) p 773
- [2] Venkatesan S, Gelatos A V, Misra V, Smith B, Islam R, Cope J, Wilson B, Tuttle D, Cardwell R, Anderson S, Angyal M, Bajaj R, Capasso C, Crabtree P, Das S, Farkas J, Filipiak S, Fiordalice B, Freeman M, Gilbert P V, Herrick M, Jain A, Kawasaki H, King C, Klein J, Lii T, Reid K, Saaranen T, Simpson C, Sparks T, Tsui P, Venkatraman R, Watts D, Weitzman E J, Woodruff R, Yang I, Bhat N, Hamilton G and Yu Y 1997 *IEEE Technical Digest on International Electronic Devices Meeting* (Washington, DC: IEEE) p 769

- [3] Edelstein D 1995 *Proc. VMIC* **12** 301
- [4] Cohen U and Tzanavaras G 2001 *Solid State Technol.* **44** 61
- [5] Gray W D and Loboda M J 2002 *Solid State Technol.* **45** 37
- [6] Reid J, Mayer S, Broadbent E, Klawuhn E and Ashtiani K 2000 *Solid State Technol.* **43** 86
- [7] Barkey D, Oberholtzer F and Wu Q 1995 *Phys. Rev. Lett.* **75** 2980
- [8] Leger C, Servant L, Bruneel J L and Argoul F 1999 *Physica A* **263** 305
- [9] Garik P, Barkey D, Ben-Jacob E, Bochner E, Broxholm N, Miller B, Orr B and Zamir R 1989 *Phys. Rev. Lett.* **62** 2703
- [10] Melrose J R, Hibbert D B and Ball R C 1990 *Phys. Rev. Lett.* **65** 3009
- [11] Fleury V, Chazalviel J N and Rosso M 1992 *Phys. Rev. Lett.* **68** 2492
- [12] Lopez-Salvans M Q, Trigueros P P, Vallmitjana S, Claret J and Sagues F 1996 *Phys. Rev. Lett.* **76** 4062
- [13] Bradley J C, Chen H M, Crawford J, Eckert J, Ernazarova K, Kurzeja T, Lin M, McGee M, Nadler W and Stephens S G 1997 *Nature* **389** 268
- [14] Sagues F, Lopez-Salvans M Q and Claret J 2000 *Phys. Rep.* **337** 97
- [15] Wang M, Zhong S, Yin X-B, Zhou J-M, Peng R W, Wang Y and Ming N B 2001 *Phys. Rev. Lett.* **86** 3827
- [16] Fleury V and Barkey D 1996 *Europhys. Lett.* **36** 253
- [17] Fleury V, Watters W A, Allam L and Devers T 2002 *Nature* **416** 716
- [18] Devers T, Kante I, Allam L, Andrezza P and Fleury V 2004 at press
- [19] Zhong S, Wang M, Yin X-B, Zhuo J-M, Peng R W, Wang Y and Ming N-B 2001 *J. Phys. Soc. Japan* **70** 1452
- [20] Weng Y Y, Wang Y, Wang M, Zhang M Z and Wang S 2004 at press
- [21] Markov I V 1995 *Crystal Growth for Beginners: Fundamentals of Nucleation, Crystal Growth and Epitaxy* (Singapore: World Scientific)
- [22] Bohannan E W, Huang L-Y, Miller F S, Shumsky M G and Switzer J A 1999 *Langmuir* **15** 813
- [23] Switzer J A, Huang C-J, Huang L-Y, Miller F S, Zhou Y C, Raub E R, Shumsky M G and Bohannan E W 1998 *J. Mater. Res.* **13** 909